

Supporting Information

Yolk-shelled cathode materials with extremely high electrochemical performances prepared by spray pyrolysis

Seung Ho Choi, Young Jun Hong, and Yun Chan Kang*

Department of Chemical Engineering, Konkuk University, 1 Hwayang-dong, Gwangjin-gu,
Seoul 143-701, Korea

This file includes:

- TEM images of the yolk-shell $\text{LiNi}_{0.5}\text{Mn}_{1.5}\text{O}_4$ powders prepared directly by spray pyrolysis process.
- TEM and FE-SEM images of the yolk-shell $\text{LiNi}_{0.5}\text{Mn}_{1.5}\text{O}_4$ cathode materials post-treated at 700°C and 750°C.
- XRD patterns of the yolk-shell-structured $\text{LiNi}_{0.5}\text{Mn}_{1.5}\text{O}_4$ powders post-treated at various temperatures.
- Cycle performances of the yolk-shell-structured $\text{LiNi}_{0.5}\text{Mn}_{1.5}\text{O}_4$ powders post-treated at various temperatures at a constant charge/discharge rate of 10 C.
- Discharge curves at extremely high discharge rates related to Fig. 4b.
- Nyquist plots of the yolk-shell $\text{LiNi}_{0.5}\text{Mn}_{1.5}\text{O}_4$ powders post-treated at 600, 700, and 750°C after first charging.
- FE-SEM images of single-crystalline $\text{LiNi}_{0.5}\text{Mn}_{1.5}\text{O}_4$ nanoparticles prepared at 750°C. Cycle properties of the yolk-shell and single-crystalline $\text{LiNi}_{0.5}\text{Mn}_{1.5}\text{O}_4$ nanoparticles prepared by flame spray pyrolysis.
- SEM and TEM images of the yolk-shell $\text{LiNi}_{0.5}\text{Mn}_{1.5}\text{O}_4$ powders after 1000 cycles.

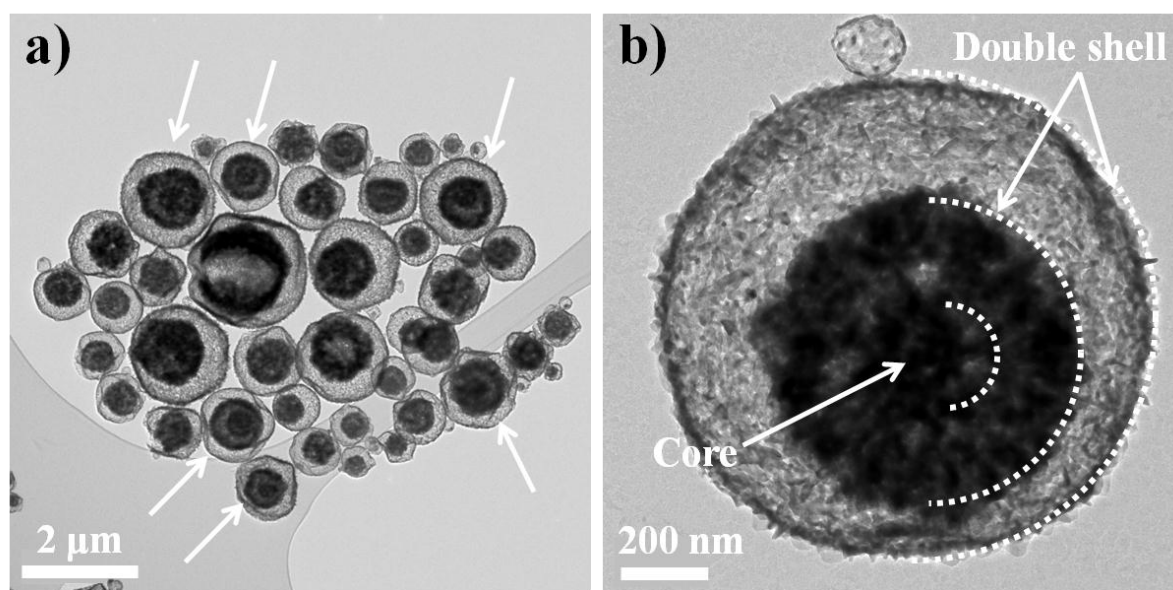


Fig. S1 TEM images of the yolk-shell $\text{LiNi}_{0.5}\text{Mn}_{1.5}\text{O}_4$ powders prepared directly by spray pyrolysis process.

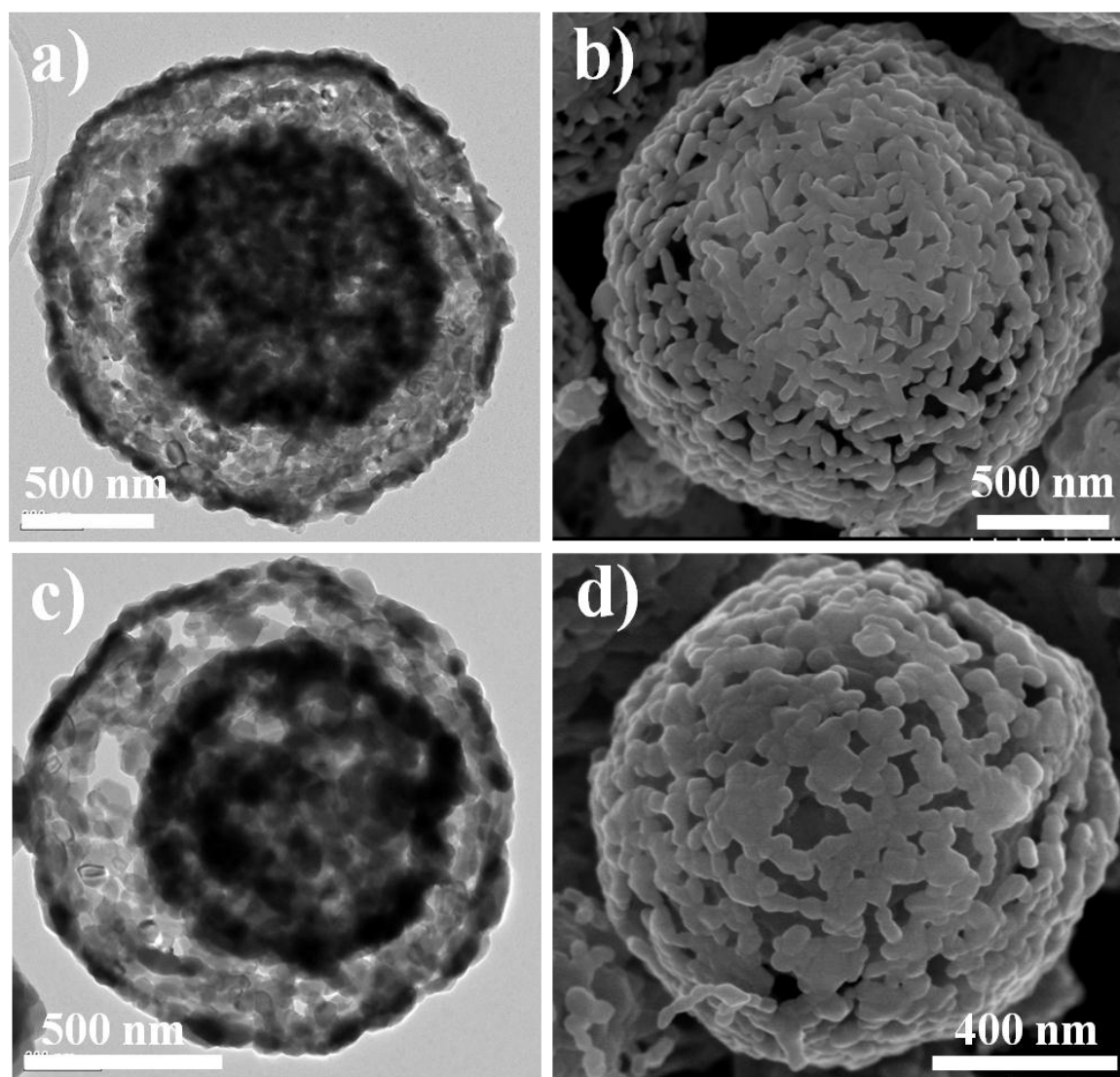


Fig. S2 TEM and FE-SEM images of the yolk-shell $\text{LiNi}_{0.5}\text{Mn}_{1.5}\text{O}_4$ cathode materials; (a,b) post-treated at 700°C , (c,d) post-treated at 750°C .

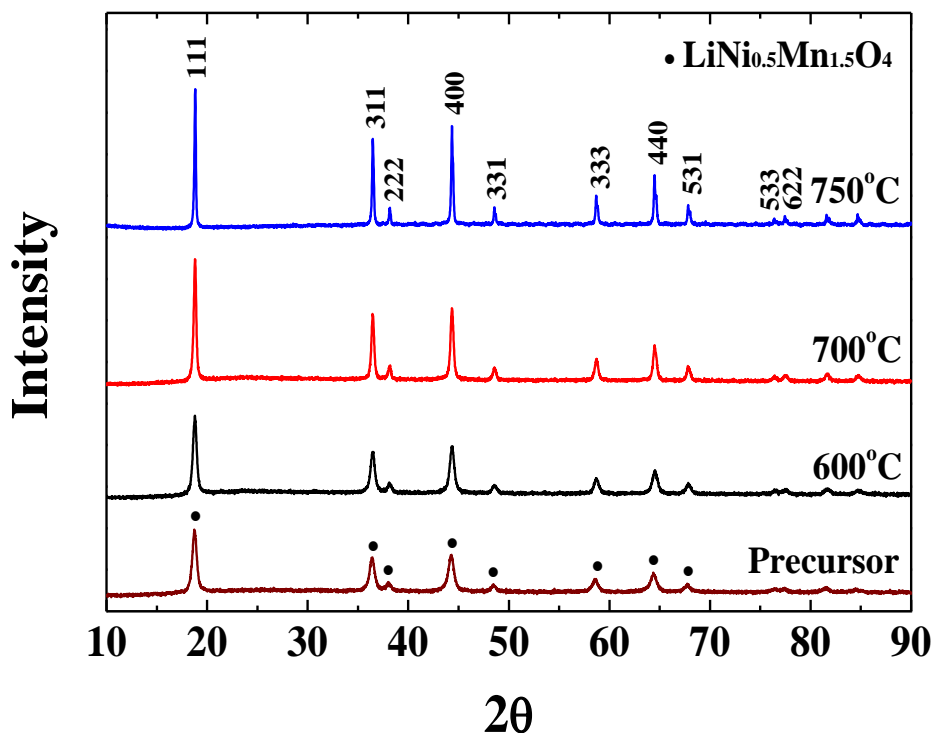


Fig. S3 XRD patterns of the yolk-shell-structured $\text{LiNi}_{0.5}\text{Mn}_{1.5}\text{O}_4$ powders post-treated at various temperatures.

The crystal structures of the yolk-shell $\text{LiNi}_{0.5}\text{Mn}_{1.5}\text{O}_4$ powders obtained before and after post-treatment are shown in Fig S3. All patterns of the precursor and post-treated powders can be assigned to cubic spinel $\text{LiNi}_{0.5}\text{Mn}_{1.5}\text{O}_4$ (JCPDS Card No.: 80-2162, space group: $F3dm$, $a = b = c = 8.170$). The mean crystallite sizes calculated using the Scherrer equation from the (111) peak widths of the precursor and post-treated powders at 600, 700, and 750°C are 16, 20, 30, and 50, respectively. A high degree of mixing of each component during drying and decomposition of droplets produced the phase pure $\text{LiNi}_{0.5}\text{Mn}_{1.5}\text{O}_4$ yolk-shell powders even at a short residence time of 4 s of the powders inside the hot wall reactor.

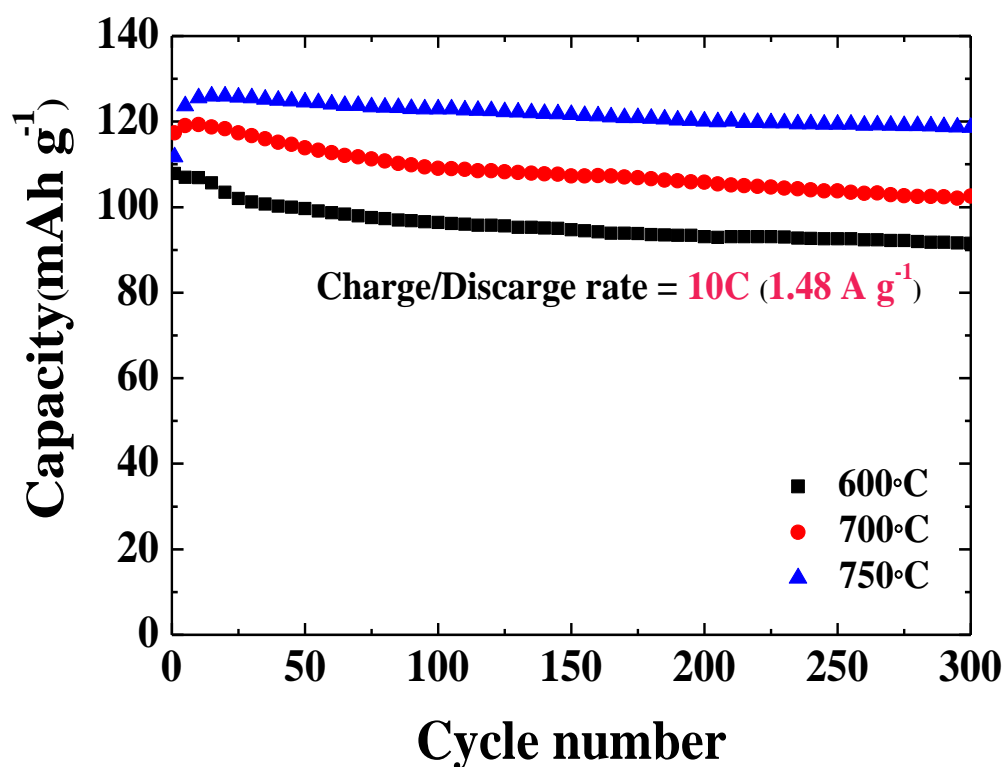


Fig. S4 Cycle performances of the yolk-shell-structured $\text{LiNi}_{0.5}\text{Mn}_{1.5}\text{O}_4$ powders post-treated at various temperatures at a constant charge/discharge rate of 10 C.

Fig. S4 shows the cycling performances of the yolk-shell $\text{LiNi}_{0.5}\text{Mn}_{1.5}\text{O}_4$ powders post-treated at 600, 700, and 750°C. The initial discharge capacities of the yolk-shell $\text{LiNi}_{0.5}\text{Mn}_{1.5}\text{O}_4$ powders post-treated at 600, 700, and 750°C were 108, 119, and 112 mAh g^{-1} , respectively. The discharge capacities of the powders post-treated at 750°C increased slightly from 112 to 126 mA h g^{-1} in the first ten cycles. The discharge capacity retentions of the $\text{LiNi}_{0.5}\text{Mn}_{1.5}\text{O}_4$ powders post-treated at 600, 700, and 750°C powders were 85%, 86%, and 94%, respectively, after 300 cycles at a high constant current density of 10 C.

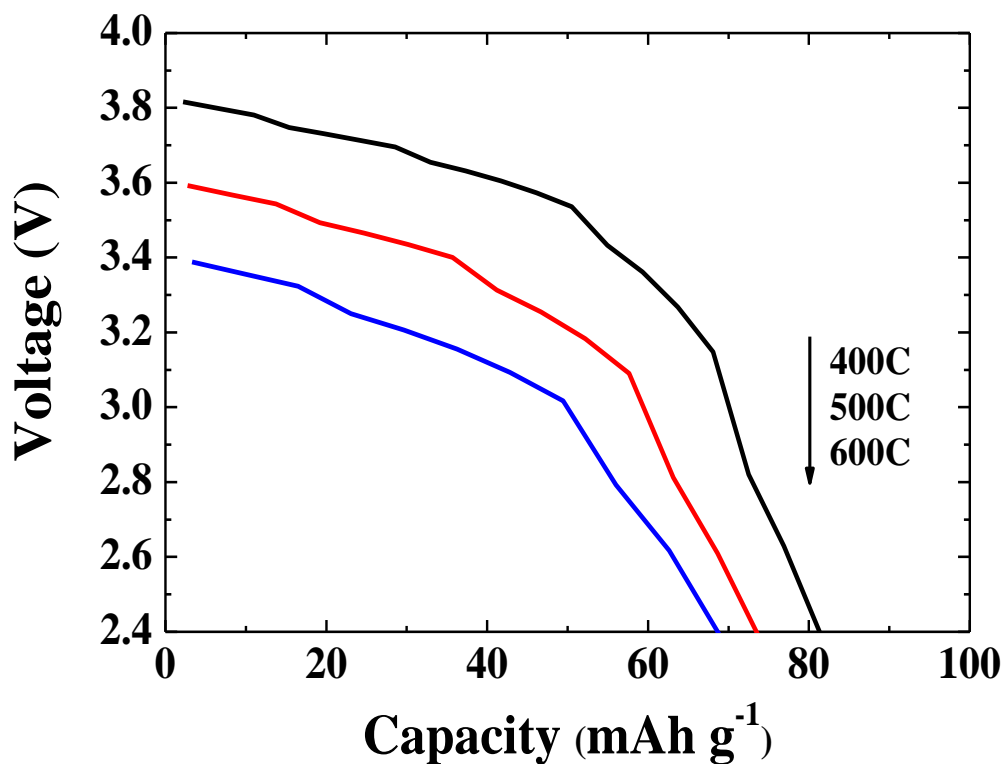


Fig. S5 Discharge curves at extremely high discharge rates related to Figure 5b.

Fig. S5 shows the discharge curves of the yolk-shell LiNi_{0.5}Mn_{1.5}O₄ powders post-treated at 750°C. As the discharge rate increases from 400 to 500, and 600 C, the discharge capacity decreases from 86 to 74, and 69 mAh g⁻¹, the corresponding energy densities are 291, 245, and 213 Wh kg⁻¹.

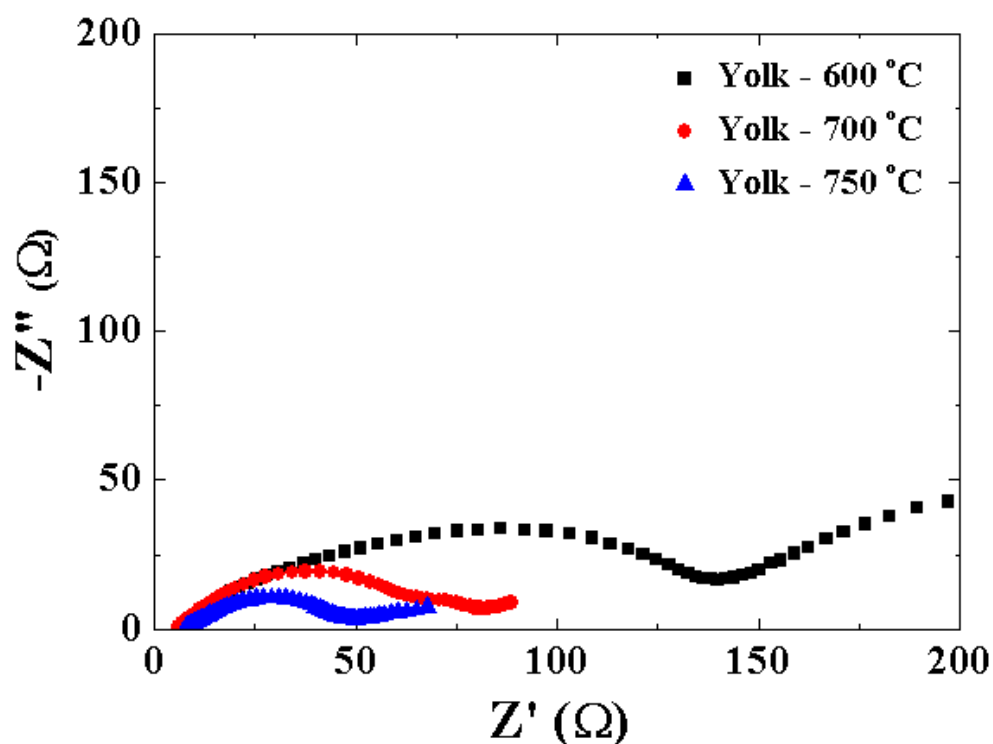


Fig. S6 Nyquist plots of the yolk-shell $\text{LiNi}_{0.5}\text{Mn}_{1.5}\text{O}_4$ powders post-treated at 600, 700, and 750 °C after first charging.

Fig. S6 shows the electrochemical impedance spectroscopy of the $\text{LiNi}_{0.5}\text{Mn}_{1.5}\text{O}_4$ yolk-shell powders post-treated at various temperatures. The medium-frequency semicircle was assigned to the charge-transfer resistance (R_{ct}) at the interface between the electrode material and the electrolyte. The charge-transfer resistances of the yolk-shell $\text{LiNi}_{0.5}\text{Mn}_{1.5}\text{O}_4$ powders post-treated at 600, 700, and 750 °C were 155, 71, and 42 Ω , respectively. The yolk-shell $\text{LiNi}_{0.5}\text{Mn}_{1.5}\text{O}_4$ powders with high crystallinity and phase homogeneity had the lowest charge-transfer resistance.

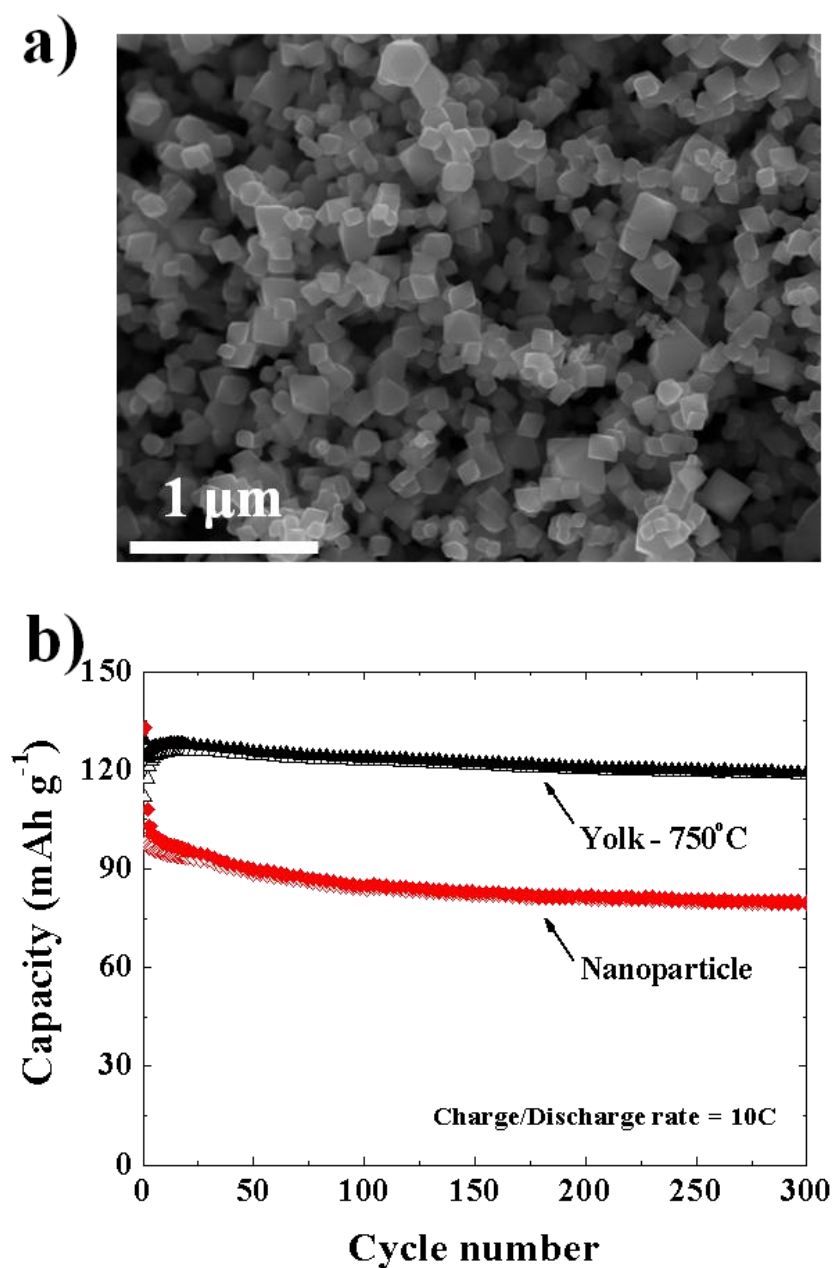


Fig. S7 (a) FE-SEM images of single-crystalline $\text{LiNi}_{0.5}\text{Mn}_{1.5}\text{O}_4$ nanoparticles prepared at 750°C . (b) Cycle properties of the yolk-shell and single-crystalline $\text{LiNi}_{0.5}\text{Mn}_{1.5}\text{O}_4$ nanoparticles prepared by flame spray pyrolysis.

The cycling performances of the yolk-shell $\text{LiNi}_{0.5}\text{Mn}_{1.5}\text{O}_4$ powders post-treated at 750°C were compared to those of the $\text{LiNi}_{0.5}\text{Mn}_{1.5}\text{O}_4$ nanopowders prepared by flame spray pyrolysis at a high current density of 10 C. Fig. S7a shows the SEM image of the $\text{LiNi}_{0.5}\text{Mn}_{1.5}\text{O}_4$ nanopowders prepared by flame spray pyrolysis. The precursor powders

directly prepared by flame spray pyrolysis were post-treated at 750°C. The detail procedure of the flame spray pyrolysis was described in our previous report [*Int. J. Electrochem. Sci.*, 2013, 8, 1146]. The $\text{LiNi}_{0.5}\text{Mn}_{1.5}\text{O}_4$ nanopowders had the mean size of 80 nm. The $\text{LiNi}_{0.5}\text{Mn}_{1.5}\text{O}_4$ nanopowders had the discharge capacities of 98 and 79 mA h g^{-1} for the 1st and 300th cycles. However, the yolk-shell $\text{LiNi}_{0.5}\text{Mn}_{1.5}\text{O}_4$ powders delivered a high discharge capacity of 119 mA h g^{-1} after 300 cycles. The yolk-shell $\text{LiNi}_{0.5}\text{Mn}_{1.5}\text{O}_4$ powders had better cycling performance compared to that of the nanopowders at a high current density.

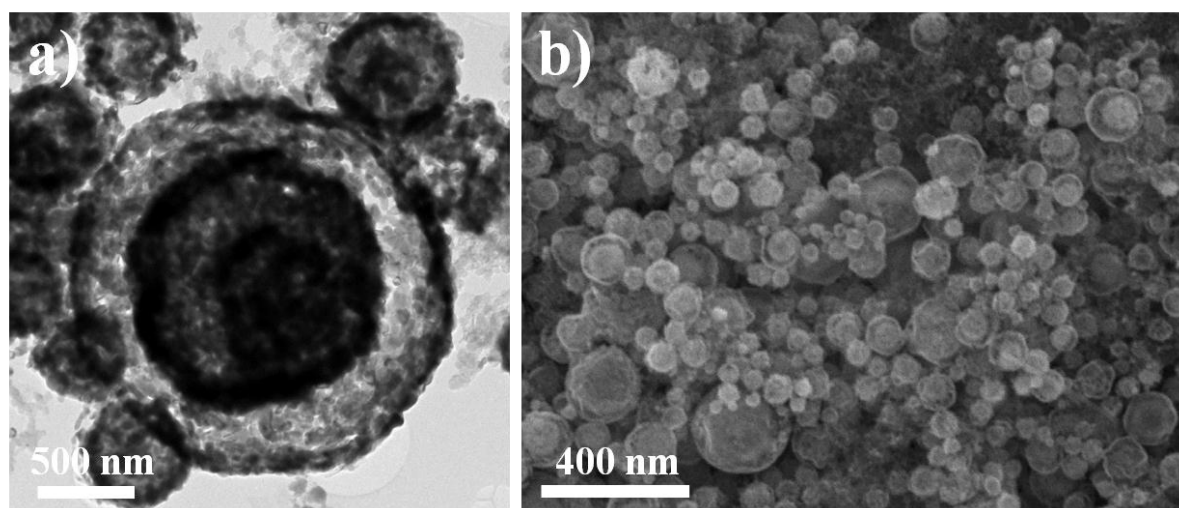


Fig. S8 SEM and TEM images of the yolk-shell $\text{LiNi}_{0.5}\text{Mn}_{1.5}\text{O}_4$ powders after 1000 cycles.

Fig. S8 shows the morphologies of the yolk-shell $\text{LiNi}_{0.5}\text{Mn}_{1.5}\text{O}_4$ powders after 1000 cycles. SEM and TEM images showed that the yolk-shell $\text{LiNi}_{0.5}\text{Mn}_{1.5}\text{O}_4$ powders maintained their overall morphology after 1000 cycles.